

# Fluorine Substitution Can Block CYP3A4 Metabolism-Dependent Inhibition: Identification of (*S*)-*N*-[1-(4-Fluoro-3-morpholin-4-ylphenyl)ethyl]-3-(4-fluorophenyl)acrylamide as an Orally Bioavailable KCNQ2 Opener Devoid of CYP3A4 Metabolism-Dependent Inhibition

Yong-Jin Wu,<sup>\*,†</sup> Carl D. Davis,<sup>‡</sup> Steven Dworetzky,<sup>||</sup> William C. Fitzpatrick,<sup>§</sup> David Harden,<sup>§</sup> Huan He,<sup>†</sup> Ronald J. Knox,<sup>§</sup> Amy E. Newton,<sup>||</sup> Thomas Philip,<sup>‡</sup> Craig Polson,<sup>||</sup> Digavalli V. Sivarao,<sup>||</sup> Li-Qiang Sun,<sup>†</sup> Svetlana Tertysnikova,<sup>||</sup> David Weaver,<sup>§</sup> Suresh Yeola,<sup>‡</sup> Mary Zoekler,<sup>‡</sup> and Michael W. Sinz<sup>‡</sup>

Bristol-Myers Squibb Pharmaceutical Research Institute,  
5 Research Parkway, Wallingford, Connecticut 06492

Received May 23, 2003

**Abstract:** The formation of a reactive intermediate was found to be responsible for CYP3A4 metabolism-dependent inhibition (MDI) observed with (*S*)-*N*-[1-(3-morpholin-4-ylphenyl)ethyl]-3-phenylacrylamide (**1**). Structure-3A4 MDI relationship studies culminated in the discovery of a difluoro analogue, (*S*)-*N*-[1-(4-fluoro-3-morpholin-4-ylphenyl)ethyl]-3-(4-fluorophenyl)acrylamide (**2**), as an orally bioavailable KCNQ2 opener free of CYP3A4 MDI.

CYP3A4 is a major CYP450 isoform and accounts for 30% of total CYP protein in human liver. CYP3A4 has a broad substrate specificity and is estimated to be involved in the metabolism of approximately 50% of drugs used in humans. Coadministered CYP3A4 inhibitors such as ketoconazole and ritonavir are a major concern in both drug development and clinical practice by virtue of this enzyme's involvement in the clearance of a majority of drugs. Hence it is common practice to screen a new chemical entity for its potential to inhibit CYP3A4.<sup>1</sup>

Recently, we reported the discovery of (*S*)-*N*-[1-(3-morpholin-4-ylphenyl)ethyl]-3-phenylacrylamide (**1**, Chart 1) as a novel KCNQ2 potassium channel opener with excellent oral bioavailability in dogs and rats.<sup>2</sup> This compound demonstrated significant oral activity in a cortical spreading depression model of migraine, suggesting that KCNQ2 openers may have potential for the treatment of some types of migraine headache.<sup>3</sup> To assess the potential likelihood of drug–drug interactions, we evaluated the cytochrome P450 inhibitory potential of **1** using recombinant (r) CYP1A2, CYP2C9, CYP2C19, CYP2D6, and CYP3A4 (Table 1). Low to moderate levels of inhibition were observed with several major human P450 enzymes with the most potent inhibition seen against CYP2C9 (IC<sub>50</sub> 5.3 μM). In subsequent medium-throughput time dependent inhibi-

## Chart 1

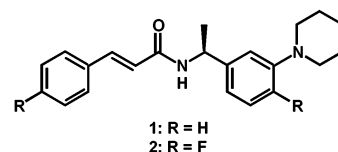


**Table 1.** Human Cytochrome P450 Inhibitory Potential of **1** with Recombinant Human CYP450 Enzymes

CYP	1A2	2C9	2C19	2D6	3A4 <sup>b</sup>	3A4 <sup>c</sup>
IC <sub>50</sub> (μM) <sup>a</sup>	78	5.3	13	>100	27	76

<sup>a</sup> IC<sub>50</sub> values were determined for inhibition of deethylation of 3-cyano-7-ethoxycoumarin (CYP1A2 and CYP2C19), dealkylation of 7-methoxy-4-trifluoromethylcoumarin (CYP2C9) and for inhibition of demethylation of 3-[2-(*N,N*-diethyl-*N*-methylamino)ethyl]-7-methoxy-4-methylcoumarin (CYP2D6). Two different substrates were used to determine the IC<sub>50</sub> values for CYP3A4; the inhibition of dealkylation of BzRes (benzoylresorufin) and of BFC (7-benzyloxy-4-trifluoromethylcoumarin). These values are the mean of duplicate determinations. <sup>b</sup> BFC used as the substrate. <sup>c</sup> BzRes as the substrate.

**Table 2.** Time-Dependent Inhibition Changes of **1** and **2** Using rCYP3A4 and BFC (IC<sub>50</sub>, μM)

compound	5 min	15 min	30 min	45 min
<b>1</b>	96	62	33	22
<b>2</b>	18	21	19	19
troleandomycin	61	33	20	16
ketoconazole	0.016	0.013	0.017	0.022

tion (TDI) studies, no TDI was observed with rCYP2C9. However, when rCYP3A4 was used, compound **1** resulted in an approximate 4-fold decrease in IC<sub>50</sub> between 5 and 45 min, while a 3.8-fold decrease and a 1.4-fold increase were observed for our reference compounds: troleandomycin (a potent metabolism dependent CYP3A4 inhibitor) and ketoconazole (a potent reversible, non-metabolism dependent CYP3A4 inhibitor), respectively (Table 2).<sup>4</sup> In our assay, compounds with 2-fold decrease or more in IC<sub>50</sub> between 5 and 45 min are defined as time-dependent inhibitors. To confirm the CYP3A4 time-dependent inhibition observation and further characterize the inhibition mechanism as metabolism dependent, compound **1** (100 μM) was preincubated with human liver microsomes in the presence of NADPH. Microsomal aliquots were taken at various time points and diluted 20-fold in a second assay that measured testosterone 6β-hydroxylation as an indication of CYP3A4 enzyme activity (Figure 1). Both fluoxetine and troleandomycin, known MDI's, were included as positive controls. The preincubation–dilution experiment (described above) was also carried out in human liver microsomes at multiple concentrations of compound **1**. Figure 2 shows that the CYP3A4-MDI was observed at all concentrations tested and especially salient at higher concentrations. Furthermore, the inhibitory effect on CYP3A4 activity was not eliminated after dialysis of the above microsomal incubations, thereby significantly reducing the possibility of reversible inhibition caused by formation of an inhibitory metabolite. Thus, the CYP3A4 MDI could arise from either mechanism-based inactivation or quasi-irreversible inhibition.

It is well-known that compounds with dialkylamine functionality undergo sequential dealkylation–oxidation

\* Corresponding author. Tel.: +1-203-677-7485; fax: +1-203-677-7702; e-mail: yong-jin.wu@bms.com.

<sup>†</sup> Department of Neuroscience Chemistry.

<sup>‡</sup> Department of Preclinical Candidate Optimization.

<sup>||</sup> Department of Neuroscience Biology.

<sup>§</sup> Department of New Leads Biology.

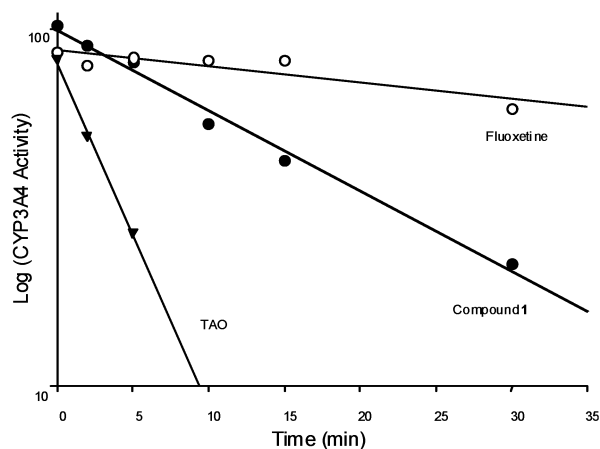


**Figure 1.** Metabolism and time-dependent inhibition of **1**, troleandomycin (TAO), and fluoxetine in human liver microsomes (all compounds at 100  $\mu$ M).

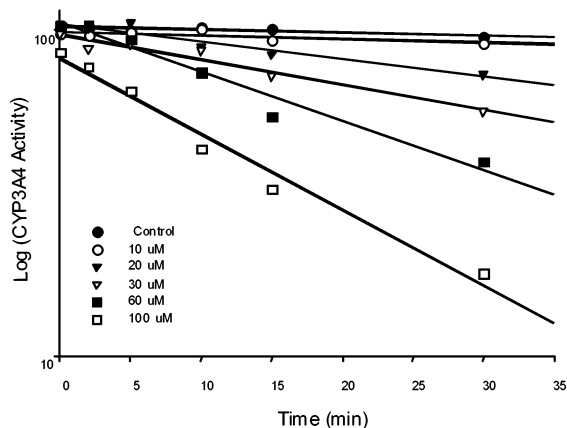


**Figure 2.** Metabolism and time-dependent inhibition of **1** in human liver microsomes at various concentrations. Testosterone  $6\beta$ -hydroxylation used as an indication of CYP3A4 enzyme activity.

reactions leading to formation of a nitroso intermediate. This reactive intermediate can coordinate in a quasi-irreversible fashion with the prosthetic heme iron of CYP3A4 leading to formation of a catalytically inactive metabolite-intermediate complex (MIC) with the enzyme. Macrolide antibiotics such as erythromycin, clarithromycin, and troleandomycin are typical examples of drugs that form MIC's.<sup>5</sup> However, no evidence of a MIC was demonstrated in the rCYP3A4 binding spectrum of **1**, where troleandomycin and fluoxetine were employed as positive controls (data not shown). We also investigated the effect of potential modifiers, such as glutathione and catalase, on the inactivation of CYP3A4 when incubated with human liver microsomes and **1** (100  $\mu$ M), and no significant differences were observed in their presence (<15% difference in the degree of enzyme inactivation), suggesting that the process was likely confined to the CYP3A4 active site and did not involve peroxidative reactions outside of the active site. Multiple enzymes can be involved in the metabolism of a substrate as well as its clearance and the formation of potential inhibitory metabolites. In this case, isoform-selective chemical inhibition studies in human liver microsomes (Figure 3) showed that CYP3A4 is a major CYP450 responsible for the metabolism of **1** as indicated by the decrease in the extent of metabolism by the CYP3A4 inhibitor ketoconazole.

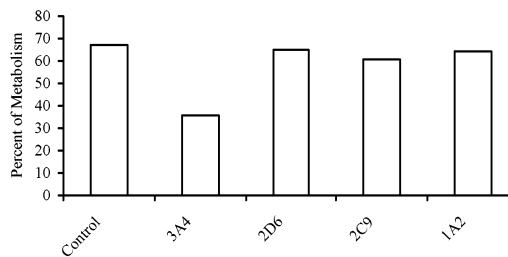
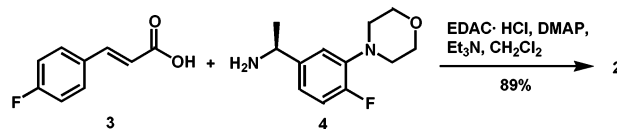


**Figure 3.** Effect of CYP isoform-selective inhibitors on the extent of metabolism of compound **1** in human liver microsomes during a 60 min incubation. Inhibitors: 2  $\mu$ M ketoconazole for 3A4; 2  $\mu$ M quinidine for 2D6; 20  $\mu$ M sulphenazole for 2C9; 25  $\mu$ M furafylline for 1A2.

### Scheme 1

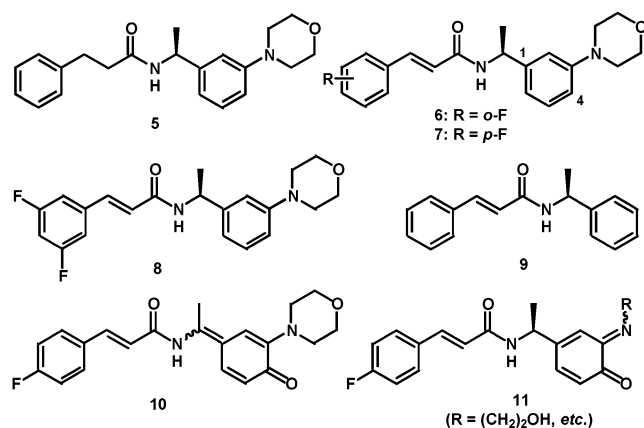


Taken together, these data suggests that compound **1** is metabolized by CYP3A4 to form a reactive intermediate. This intermediate appears to be restricted to the CYP3A4 active site and covalently binds to the CYP3A4 enzyme, leading to irreversible enzyme inactivation, also called mechanism-based inactivation. This type of inhibition is viewed as an undesirable characteristic since the degree of inhibition extends beyond the elimination of the drug and may increase with multiple dosing, thus leading to serious drug–drug interactions. Moreover, compounds with potent irreversible inhibition characteristics can exhibit nonlinear pharmacokinetics.<sup>6</sup> For these reasons, we chose to develop a new analogue with KCNQ2 opener activity and a pharmacokinetic profile comparable to **1**, but devoid of 3A4 MDI. This report describes the discovery of acrylamide **2** (Chart 1) that appears to meet the above criteria.

The synthesis of acrylamide **2** is shown in Scheme 1. Coupling of (*S*)-1-(4-fluoro-3-morpholin-4-ylphenyl)ethylamine (**4**)<sup>7</sup> with 3-(4-fluorophenyl)acrylic acid (**3**) in the presence of 1-(3-dimethylaminopropyl)-3-ethylcarbodiimide hydrochloride (EDAC·HCl), 4-(dimethylamino)pyridine (DMAP) and triethylamine afforded **2** in good yield.

The structure-3A4 MDI relationship studies were carried out to identify the possible site(s) responsible for the generation of the reactive intermediate described above for compound **1**. Reduction of the  $\alpha,\beta$ -unsaturated double bond (i.e., **5**, Chart 2) or fluoro substitution of the phenyl on the left (i.e., **6**, **7**, and **8**) did not eliminate the CYP3A4 MDI (using the rCYP3A4-BFC assay), suggesting that the reactive intermediate may be formed on the *N*-phenylmorpholine moiety of **1**. Since CYP3A4 MDI was not observed with compound **9**, the morpholinyl group must play a role in the formation of the reactive intermediate on the *N*-phenylmorpholine moiety. Monohydroxylation of this moiety was seen in the biotransformation of **1** with both human or rat liver microsomes. To block the potential hydroxylation of the phenyl ring on the right, we substituted the hydrogen attached to C4 (see Chart 2) with a fluorine<sup>8</sup> as this position appears to be most susceptible to hydroxylation based on electronic and steric considerations. Among a

## Chart 2



series of 4-fluoro-substituted analogues synthesized, acrylamide **2** was found to exhibit comparable KCNQ2 opener activity to **1** (vide infra) and yet no CYP3A4 MDI, as shown in Table 2. The lack of CYP3A4 MDI observed with the difluoro compound **2** is due to the fluorine adjacent to the morpholinyl group, not the fluorine attached to the phenyl on the left (styrene), since the monofluoro analogue **7** displayed CYP3A4 MDI (3.6-fold decrease in IC<sub>50</sub> between 5 and 20 min). Presumably, 4-fluoro substituent can prevent hydroxylation at this position, thus blocking the formation of a reactive quinone intermediate such as **10** or **11**.<sup>9</sup> Further studies are required to establish the exact reactive intermediate.

The concentration response effects of **2** were determined on mKCNQ2 channels heterologously expressed in HEK 293 cells using the whole-cell patch-clamp recording technique as described previously.<sup>2</sup> The membrane potential of individual cells was voltage-clamped to  $-40$  mV, resulting in the generation of a maintained, steady-state baseline KCNQ2 current of  $\sim 100$  pA. Next, increasing concentrations of **2** were locally superfused onto the cells, causing a large increase in the amount of KCNQ2 current measured at  $-40$  mV. The maximal steady-state current amplitude produced by each concentration of **2** was measured and used to construct the concentration response curve shown in Figure 4. The EC<sub>50</sub>, estimated from the single binding site model logistic fit to these data, is  $1.2 \mu\text{M}$ , comparable to that obtained with **1** (about  $3 \mu\text{M}$ ).<sup>2</sup>

The effects of **2** on membrane potential were also investigated using the fluorescent membrane potential assay in SH-SY5Y human neuroblastoma cells<sup>10</sup> expressing native KCNQ channels. The relative fluorescence intensity change was used as an indication of the change in membrane potential.<sup>11</sup> As shown in Figure 5, application of **2** led to a concentration-dependent hyperpolarization of the cells. The calculated EC<sub>50</sub> of this compound is  $1.55 \mu\text{M}$ , again similar to that obtained with **1** ( $0.69 \mu\text{M}$ ).<sup>2</sup>

Compound **2** was characterized in several pharmacokinetic studies (Table 3). Oral absorption was rapid in the rat with a peak concentration occurring within 0.66 h. In iv dosing studies the compound demonstrated a moderate plasma clearance and a relatively long elimination half-life. The oral bioavailability measured was 84%, when **2** was administered as a suspension. Compound **2** was also shown to be present in brain

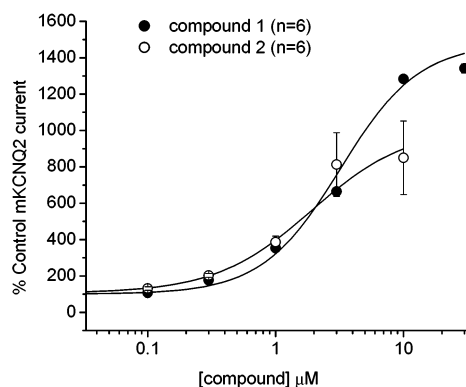


**Figure 4.** Concentration–response effects of **1** and **2** on steady-state mKCNQ2 current produced by voltage-clamping the cell membrane potential to  $-40$  mV. Data sets are the mean  $\pm$  SEM, and they are fitted with one-site model logistic functions.

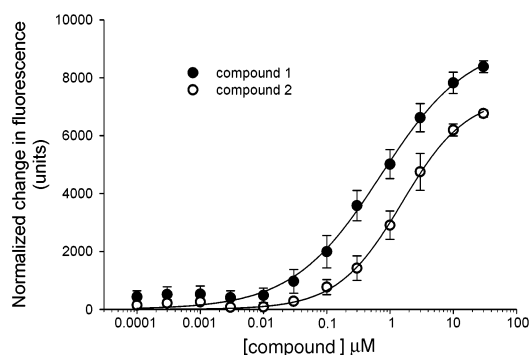


**Figure 5.** Effects of **1** and **2** on resting membrane potential in SH-SY5Y human neuroblastoma cells ( $n = 4$ ).

**Table 3.** Pharmacokinetic Parameters of **2** in the Rat

PK parameter	rat
iv <sup>a</sup>	
dose (mg/kg)	1
$t_{1/2}$ (h)	3.5
CL (mL/min/kg)	17.8
$V_d$ (L/kg)	3.3
po (suspension) <sup>b</sup>	
dose (mg/kg)	10
$t_{max}$ (h)	0.66
$F$ (%)	84

<sup>a</sup> Compound dosed to Sprague–Dawley male rats as an iv solution in PEG 400 ( $n = 3$ ). <sup>b</sup> dosed as an oral suspension in 25% PEG 400/0.5% Tween 80/74.5% pH 3 water ( $n = 3$ ).

tissue when dosed orally at 8 mg/kg in 95% PEG 400/5% DMSO in rats ( $\sim 1 \mu\text{M}$  concentration of **2**).

Compound **2** was examined for its ability to reduce the total number of cortical spreading depressions<sup>12</sup> (CSD) following intravenous administration. CSD was produced by a 10 min application of crystalline potassium chloride to a small region in the rat parietal cortex. Topical application of crystalline potassium chloride produced a continuous train of slow negative excursions in the cortical surface potential in all animals tested. The total number of depolarizations in the distal lead of each animal was used to determine the mean number of depolarizations for each group. The mean depolarizations for the vehicle-treated group was  $26.4 \pm 0.9$  ( $n = 8$ ), while the corresponding group mean for **2** treated rats was  $19.8 \pm 1.9$  ( $n = 8$ ). This approximately 25% attenuation in depolarizations in the drug-treated group was significant ( $p = 0.009$ ; two-tailed Student  $t$ -test).

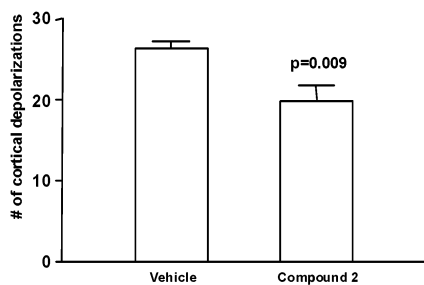


**Figure 6.** Effect of a single dose of **2** (1 mg/kg, iv) on KCl-induced cortical depolarizations. Mean depolarizations in the distal lead from individual rats organized as columns based on treatment. Horizontal bar represents the group mean  $\pm$  SEM. Inter group comparison was made using the Student's two-tailed *t*-test;  $p < 0.05$  was deemed significant.

Thus, acrylamide **2** even at 1 mg/kg (iv) produced a significant reduction on the total number of depolarization events.

In summary, the CYP3A4 MDI of **1** was eradicated through specific fluorine substitution, and the difluoro acrylamide **2** was identified as a new KCNQ2 opener<sup>13</sup> with comparable activity to **1**, but devoid of CYP3A4 MDI. Compound **2** showed the same excellent oral bioavailability in rats as compound **1** and demonstrated significant in vivo activity in a cortical spreading depression model of migraine. Thus, **2** may have potential for the treatment of some types of migraine headache with reduced likelihood of CYP3A4 inhibition related drug–drug interactions.

**Acknowledgment.** We thank the Discovery Profiling group of Bristol-Myers Squibb company (Wallingford, CT) for the P450 inhibition data.

**Supporting Information Available:** Experimental details for the synthesis of **2** and descriptions of the cortical spreading depression studies and CYP450 enzyme inhibition assays. This material is available free of charge via the Internet at <http://pubs.acs.org>.

## References

- (1) Kumar, G. N.; Surapaneni, S. Role of Drug Metabolism in Drug Discovery and Development. *Med. Res. Rev.* **2001**, *21*, 397–411.
- (2) Wu, Y.-J.; Boissard, C. G.; Greco, C.; Gribkoff, V. K.; Harden, D. G.; He, H.; L'Heureux, A.; Kang, S. H.; Kinney, G. G.; Knox, R. J.; Natale, J.; Newton, A. E.; Lehtinen-Oboma, S.; Sinz, M. W.; Sivarao, D. V.; Starrett, J. E., Jr.; Sun, L.; Tertyshnikova, S.; Thompson, M. W.; Weaver, D.; Wong, H. S.; Zhang, L.; and Dworetzky, S. I. (S)-N-[1-(3-Morpholin-4-ylphenyl)ethyl]-3-phenyl-acrylamide: an Orally Bioavailable KCNQ2 Opener with Significant Activity in a Cortical Spreading Depression Model of Migraine. *J. Med. Chem.* **2003**, *46*, 3197–3200.
- (3) For reviews on potassium channels, see: (a) Coghlan, M. J.; Carroll, W. A.; Gopalakrishnan, M. Recent Developments in the Biology and Medicinal Chemistry of Potassium Channel Modulators: Update from a Decade of Progress. *J. Med. Chem.* **2001**, *44*, 1627–1653. (b) Shieh, C.; Coghlan, M.; Sullivan, J. P.; Gopalakrishnan, M. Potassium Channels: Molecular Defects, Diseases, and Therapeutic Opportunities. *Pharmacol. Rev.* **2000**, *52*, 557–593.
- (4) For reviews on the methods and interpretation of irreversible inhibitors, see: (a) Yan, Z.; Rafferty, B.; Caldwell, G. W.; Masucci, J. A. Rapidly Distinguishing Reversible and Irreversible CYP450 Inhibitors by Fluorometric Kinetic Analyses. *Eur. J. Drug Metab. Pharmacok.* **2002**, *27*, 281–287. (b) Guengerich, F. P. in Handbook of Drug Metabolism. *Inhibition of Drug Metabolizing Enzymes: Molecular and Biochemical Aspects*; Woolf, T. F., Ed.; Marcel Dekker: New York, 1999; p 203. (c) Jones, D. R.; Hall, S. D. in Drug Drug Interactions. *Mechanism-Based Inhibition of Human Cytochrome P450: In Vitro Kinetics and In Vitro-In Vivo Correlations*; Rodrigues, A. D., Ed.; Marcel Dekker: New York, 2002; p 387.
- (5) Pershing, L. K.; Franklin, M. R. Cytochrome P-450 Metabolic-Intermediate Complex Formation and Induction by Macrolide Antibiotics; a New Class of Agents. *Xenobiotica* **1982**, *12*, 687–699.
- (6) For reviews on the impact of irreversible inhibitors, see: (a) Ito, K.; Iwatsubo, T.; Kanamitsu, S.; Ueda, K.; Suzuki, H.; Sugiyama, Y. Prediction of Pharmacokinetic Alterations Caused by Drug-Drug Interactions: Metabolic Interaction in the Liver. *Pharmacol. Rev.* **1998**, *50*, 387–411. (b) Lin, J.; Lu, A. Y. H. Role of Pharmacokinetics and Metabolism in Drug Discovery and Development. *Pharmacol. Rev.* **1997**, *49*, 403–449. (c) Jang, G.; Harris, R. Z.; Lau, D. T. Pharmacokinetics and Its Role in Small Molecule Drug Discovery Research. *Med. Res. Rev.* **2001**, *21*, 382–396.
- (7) Wu, Y.-J.; He, H.; Sun, L. Q.; Wu, D. D.; Gao, Q.; Li, H. Y. Synthesis of Fluorinated 1-(3-Morpholin-4-yl-phenyl)-ethylamines. *Bioorg. Med. Chem. Lett.* **2003**, *13*, 1725–1728.
- (8) (a) Welch, J. T.; Eshwarakrishnan, S. *Fluorine in Bioorganic Chemistry*; John Wiley and Sons: New York, 1991. (b) Kirk, K. L. Fluorine Substitution as a Modulator of Biological Processes. In *Biomedical Chemistry, Applying Chemical Principles to the Understanding and Treatment of Disease*; Torrence, P. F., Ed.; John Wiley & Son: New York, 2000; p 247.
- (9) For examples of reactive quinone intermediates, see (a) Marques, M. M.; Beland, F. A. Identification of Tamoxifen-DNA Adducts Formed by 4-Hydroxyltamoxifen Quinone Methide. *Carcinogenesis* **1997**, *18*, 1949–1954. (b) Woolf, T. F.; Pool, W. F.; Chang, T.; Goel, O. P.; Purchase, C. F., II; Schroeder, M. C.; Kunze, K. L.; Trager, W. F. Bioactivation and Irreversible Binding of the Cognition Activator Tachrine Using Human and Rat Liver Microsomal Preparations: Species Difference. *Drug Metab. Dispos.* **1993**, *21*, 874–882.
- (10) Tosetti, P.; Taglietti, V.; Toselli, M. J. Functional Changes in Potassium Conductances of the Human Neuroblastoma Cell Line SH-SY5Y during In Vitro Differentiation. *J. Neurophysiol.* **1998**, *79*, 648–58.
- (11) Whiteaker, K. L.; Gopalakrishnan, S. M.; Groebe, D.; Shieh, C. C.; Warrior, U.; Burns, D. J.; Coghlan, M. J.; Scott, V. E.; Gopalakrishnan, M. Validation of FLIPR Membrane Potential Dye for High Throughput Screening of Potassium Channel Modulator. *J. Biomol. Screening* **2001**, *6*, 305–312.
- (12) For a discussion on the cortical spreading depression animal model, see ref 2.
- (13) Preliminary studies using thallium(I) influx assay showed that **2**, like **1**,<sup>2</sup> also activated other members of the KCNQ family. Although these compounds activated these channels, further electrophysiological characterization is required.

JM034111V